Supplementary Materials for

Warmer Antarctic Summers in Recent Decades Linked to Earlier Stratospheric Final Warming Occurrences

Hyesun Choi[1], Hataek Kwon[2], Seong-Joong Kim[1]*, Baek-Min Kim[3*]

[1]Division of Polar Climate Sciences, Korea Polar Research Institute, Incheon, Republic of Korea.
[2]School of Earth and Environmental Sciences, Seoul National University, Seoul, Republic of Korea.
[3]Department of Environmental Atmospheric Science, Pukyong National University, Busan, Republic of Korea.

*Corresponding author. Email: seongjkim@kopri.re.kr
baekmin@pknu.ac.kr

This PDF file includes:

Supplementary Notes 1 to 4
Supplementary Figures 1 to 10
Supplementary Tables 1 to 4
Supplementary References

Except for Supplementary Figures 1, 2, and Supplementary Table 2, all analyses based on reanalysis used zonal wind, geopotential height, MSLP, and SAT data from the ERA-Interim daily dataset. This dataset covers the period from January 1, 1979, to August 31, 2018. Except for Supplementary Figures 1 and 2, all analyses based on in situ observations utilize monthly mean SAT data from January 1979 to January 2018 for 20 Antarctic stations from the Scientific Committee on Antarctic Research Reference Antarctic Data for Environmental Research database.

Supplementary Notes

Supplementary Note 1. Long-term variability in Antarctic SAT anomalies during austral wintertime

The pause in the Antarctic cooling trend does not occur in austral winter (Supplementary Figure 1); The SAT based on reanalysis (station data) shows an insignificant warming trend with 0.24 ^{o}C decade^{-1} (0.42 ^{o}C decade-1) during the pre-1999 period at the 90% confidence levels. During the post-1999 period, a warming trend with 0.2^{o}C decade^{-1} (0.07 ^{o}C decade^{-1}) is still observed, but it is slightly weaker than that during the pre-1999 period.

Supplementary Note 2. Influence of polar-cap averaged SAT anomalies on results

To identify the influence of opposite behavior between the AP region and the rest of Antarctica on results, we examined the time series of DJ-mean SAT anomalies averaged over the entire Antarctica and investigated the relation to SFWOD. Supplementary Figure 2 is equivalent to Figure 1a for Antarctica including the AP region. The SAT anomalies were averaged over 0°E-360°E and 70°S-90°S for the ERA5 reanalysis data and calculated from 20 stations located in the 0°E-360°E for the observations. The SAT anomalies based on reanalysis data (solid black line) and station observations (dashed-dotted black line) displayed a similar evolution, with a correlation coefficient of 0.76. On an interannual time scale, the two SAT anomalies from the reanalysis and observed data were related to SFWOD, with correlation coefficients of -0.27 and -0.36, respectively. The correlations with reanalysis-based SAT anomalies and observation-based SAT anomalies were not significant at the 95% confidence level, but significant at the 90% confidence level. On a decadal time scale, the SAT anomalies based on reanalysis and station observations show the cooling trends with -0.25 °C decade^{-1} and -0.17 °C decade^{-1} during the pre-1999 period, respectively. The cooling trends based on reanalysis and observed data, however, were only about half and one-third compared to the SAT anomalies trends calculated for the same period excluding the AP region (Figure 1a), respectively. Moreover, they were not significant even at both the 90% and 95% confidence levels. During the post-1999 period, the SAT anomalies based on reanalysis and station observations also show insignificant trends with 0.29 °C decade^{-1} and -0.04 °C decade^{-1} at both the 90% and 95% confidence levels, respectively. Therefore, averaging over the entire Antarctica, including the AP region, considerably reduced the cooling trends during pre-1999 periods, making it ambiguous to claim a pause in the cooling trends since 1999.

Supplementary Note 3. Choice of a turnaround year

The trends and differences for the different turnaround years (1998, 1999, 2000, and 2000) are shown in Supplementary Table 1. The reanalysis cooling trend and the trend toward the later occurrence of SFW during the SFWOD delay period remained significant for all turning points tested and ceased during the SFWOD advance period. Although the observed cooling trend during the SFW delay period was smaller than the reanalysis cooling trend, it was significant, except when 1998 was considered as the turnaround year. Supplementary Table 1 shows that trend differences are insensitive to the choice of turnaround year. We chose 1999 as the turnaround year, as 1999 was the year with the lowest SAT anomalies over Antarctica, excluding the AP region during summer and the latest SFWOD (Figure 1a); the trend differences between the two eras (1979–1999 and 1999–2017) for the SAT anomalies and SFOWD were the largest, as shown in Supplementary Table 1.

Supplementary Note 4. Close linkage between SFWOD and summer surface responses over Antarctica

Kwon et al. (2020) showed that extreme southern stratospheric polar vortex (SSPV) weakening events, which occurred often during the austral late winter and spring season (August–October), had impacts on the surface through stratosphere-troposphere coupling for approximately three months[1]. We examined the linkage not only between extreme SSPV weakening events and SFW timing but also with surface responses before December shown in Figure 5. The analysis was performed using the ERA-interim data for the period from January 1, 1979, to August 31, 2018, as employed in Kwon et al. (2020)[1]. Supplementary Figure 9 shows the composite of PCH anomalies based on the years with or without preceding extreme SSPV weakening events for early and late SFWs, respectively. Extreme SSPV weakening events were referenced from Kwon et al. (2020)'s Table 1[1], with an average onset date of September 22nd, which is about three months earlier than the average onset date of December 7th for the SFWs (Supplementary Table 4). There are two notable points. First, from the perspective of the SSPV weakening events, out of the 15 cases of the SSPV weakening events (Supplementary Figures 9a and 9c), 11 cases are followed by early SFW events (Supplementary Figure 9a), while out of the 24 cases where they do not occur (Supplementary Figures 9b and 9d), 15 cases are followed by late SFW events (Supplementary Figure 9d). Second, regardless of the timing of SFW, before mid-November, positive anomalies are observed for years with the SSPV weakening events (Supplementary Figures 9a and 9c), whereas negative anomalies are identified for years without SSPV weakening events (Supplementary Figures 9b and 9d). However, after mid-November, positive anomalies are observed during early SFW events (Supplementary Figures 9a and 9b) while negative PCH anomalies are observed during late SFW events (Supplementary Figures 9c and 9d). In other words, surface responses before mid-November are mainly associated with extreme SSPV weakening events, whereas those afterward appear to be closely linked with SFWOD.

Supplementary Figures

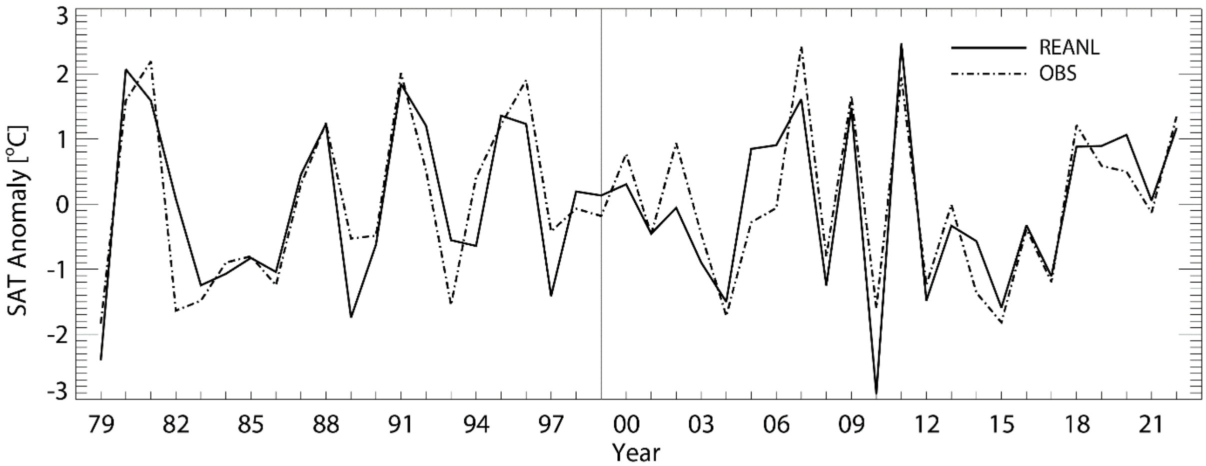

Supplementary Figure 1. **Time series of June-July-August-mean SAT anomalies averaged over Antarctica excluding the AP region.** The black solid and dashed-dotted lines correspond to the results from the reanalysis data (ERA5) and station observations, respectively. The vertical gray line represents the year 1999.

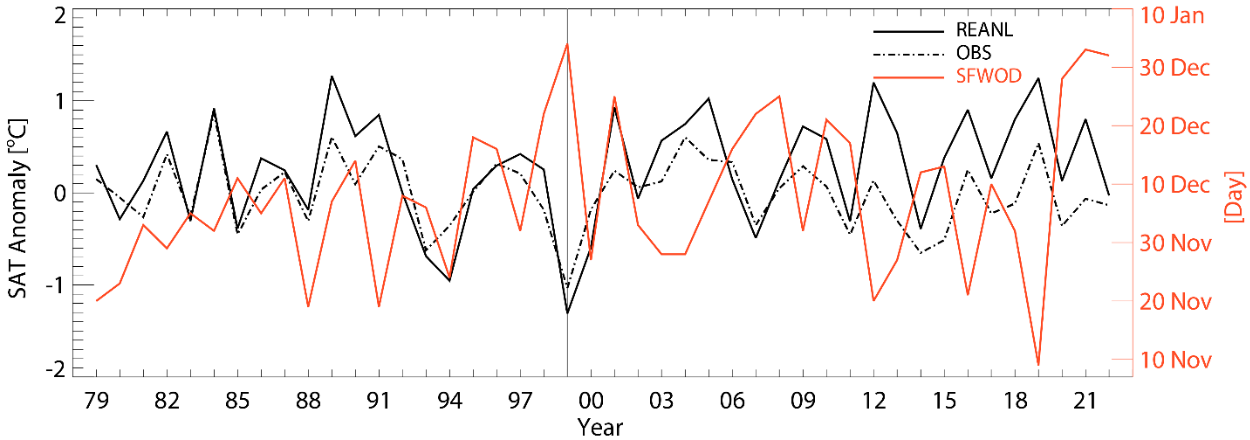

Supplementary Figure 2. Time series of DJ-mean SAT anomaly averaged over Antarctica including the AP region (black) and SFWOD (orange). The black solid and dashed-dotted lines correspond to the results from the ERA5 reanalysis data and station observations, respectively. The vertical gray line represents the year 1999. Refer to the left axis for the DJ-mean SAT anomaly and the right axis for SFWOD. SFWOD is referenced in Supplementary Table 2.

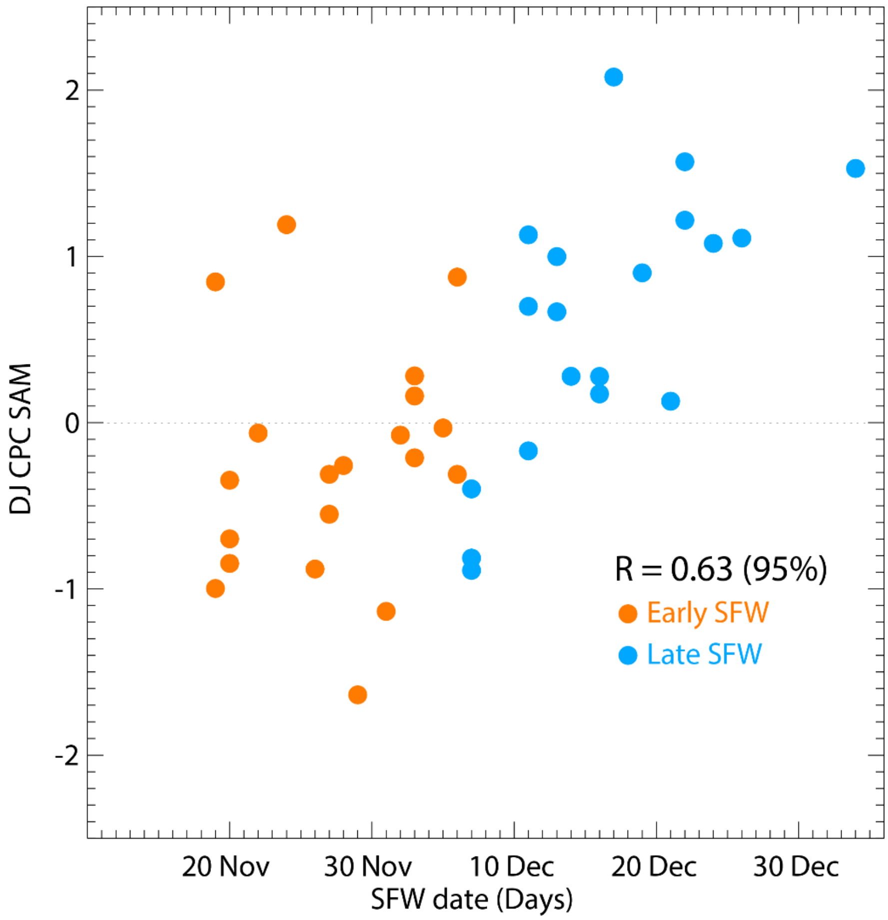

Supplementary Figure 3. Scatterplot of the SFWOD based on ERA-Interim versus the DJ-mean SAM. The orange and blue circles denote early and late SFW events, respectively. SFWOD is referenced in Supplementary Table 4. The correlation coefficients (R) and confidence levels (parentheses) are shown in the lower-right corner of the plot.

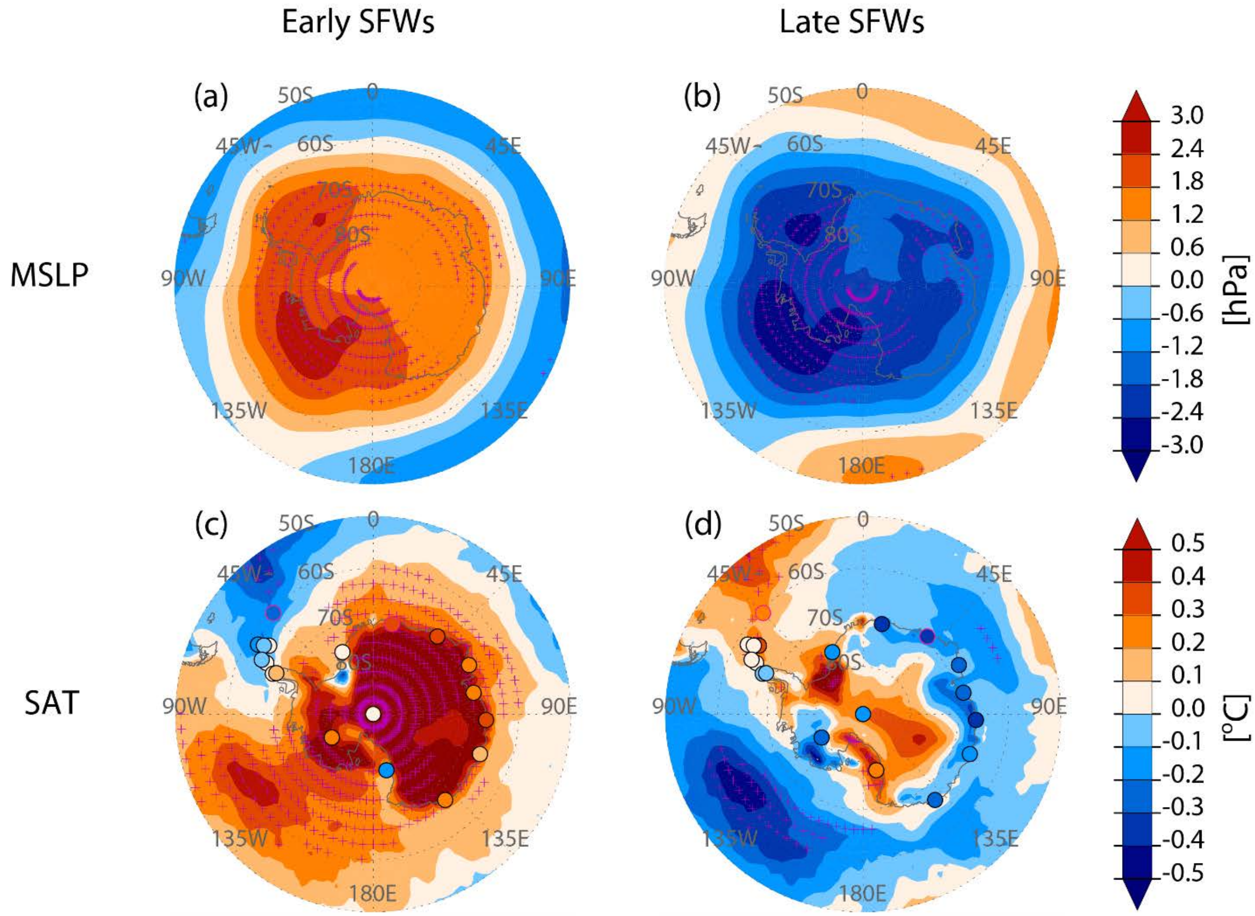

Supplementary Figure 4. Spatial distributions of MSLP and SAT anomalies according to SFWOD based on ERA-Interim. DJ-mean MSLP anomalies for (a) the early-SFW and (b) late-SFW events. (c, d) are equivalent to (a, b) for DJ-mean SAT anomalies. SFWOD is referenced in Supplementary Table 4. The circles in (c) and (d) are the SAT anomalies for 20 Antarctic stations. Pink crosses and circles indicate significance at the 95% confidence level.

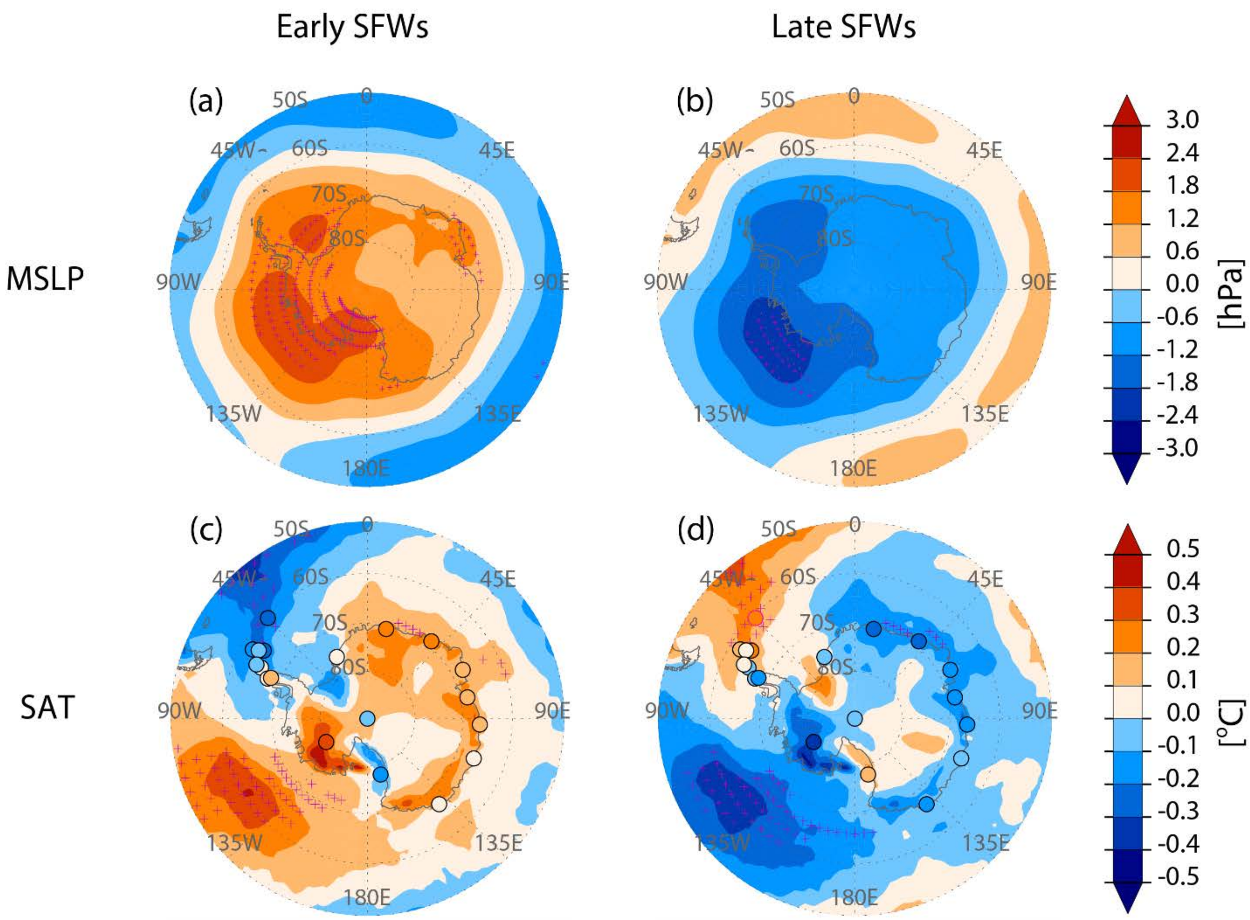

Supplementary Figure 5. Spatial distributions of detrended MSLP and detrended SAT anomalies according to SFWOD based on ERA-Interim. As in Supplementary Figure 4 but for that we first removed the piecewise linear trends separately over the SFWOD-delay and advance periods and then conducted a composite analysis according to the SFWOD.

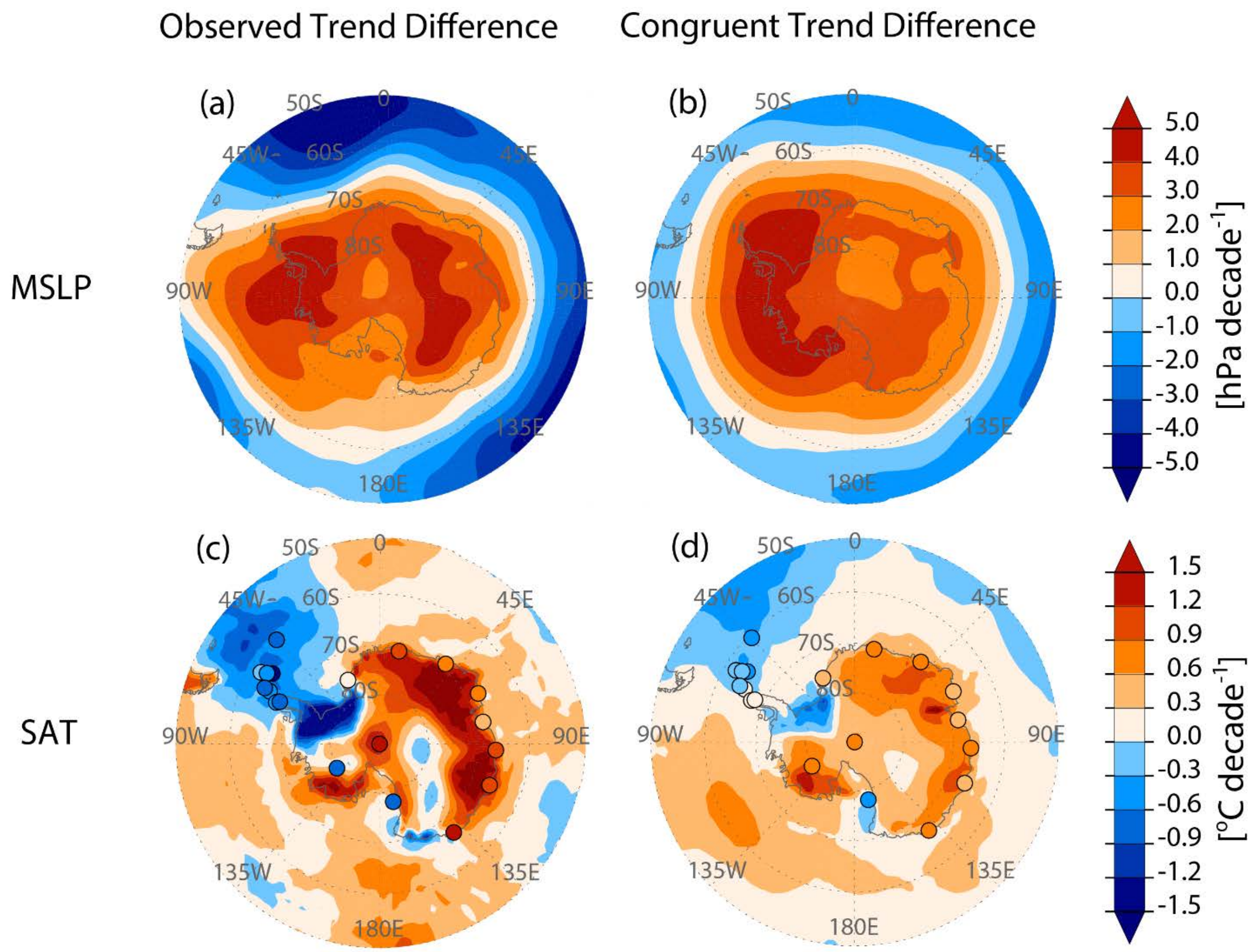

Supplementary Figure 6. **Spatial distributions of observed and congruent trend differences in MSLP and SAT anomalies based on ERA-Interim**. (a) Trend differences between SFWOD-delay (1979-1999) and advance period (1999-2017) in DJ-mean MSLP anomaly (post-1999 period minus pre-1999 period). (b) is equivalent to (a) for trends linearly congruent with SFWOD. (c) and (d) are equivalent to (a) and (b), respectively, for SAT anomalies. SFWOD is referenced in Supplementary Table 4. The circles in (c) and (d) are the DJ-mean SAT anomalies for 20 Antarctic stations.

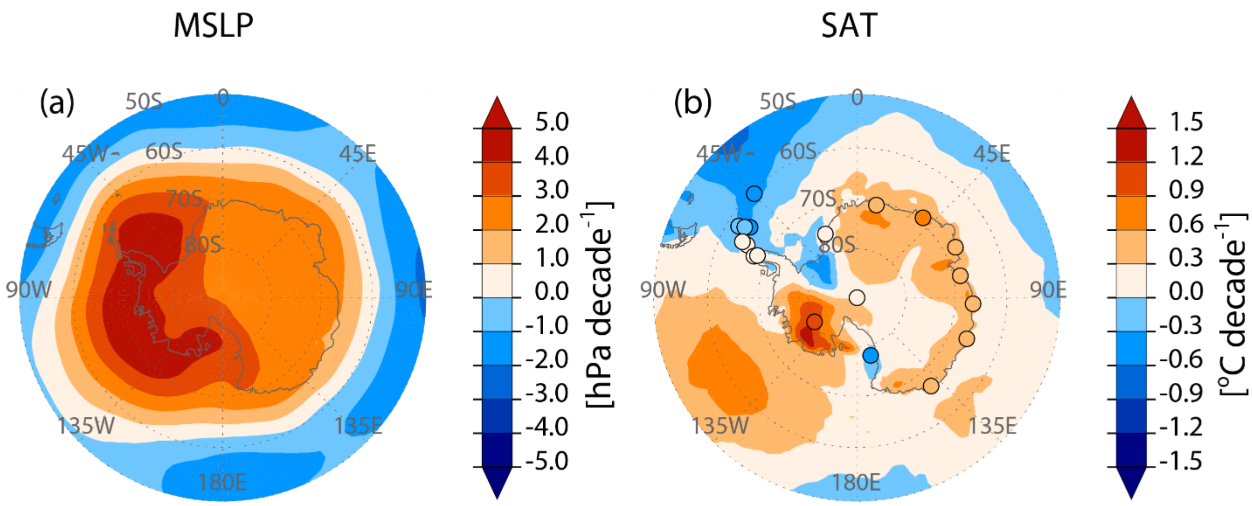

Supplementary Figure 7. Comparative analysis of Supplementary Figures 6b and 6d. (a) and (b) are equivalent to Supplementary Figures 6b and 6d, respectively, but for that, for the SFWOD index and the two atmospheric variables, we first removed the piecewise linear trends separately over the SFWOD-delay (1979-1999) and advance (1999-2017) periods, calculated the regression map for the entire period, and then multiplied the same regression map by the SFWOD trend for each period separately.

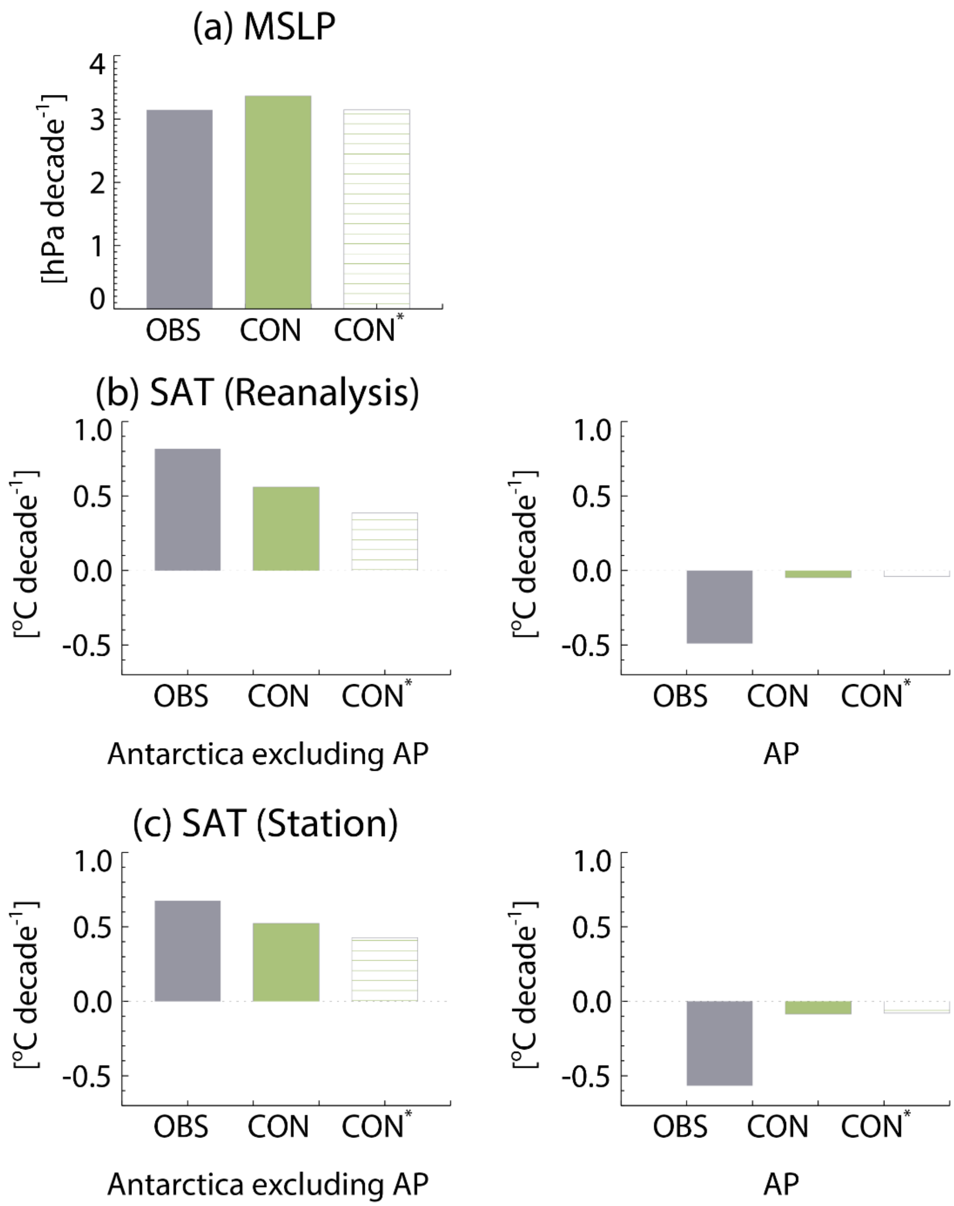

Supplementary Figure 8. Trend differences in MSLP and SAT anomalies between SFWOD-delay and advance periods: a comparative analysis using original observations and linear congruence with SFWOD. (a) Trend differences between SFWOD-delay and advance periods in the DJ-mean MSLP anomaly (post-1999 period minus pre-1999 period). The results from the original observation are represented by the gray solid color (OBS) bar, while the green solid color (CON) and green parallel line (CON*) bars indicate the results that are linearly congruent with SFWOD using regression maps calculated with non-detrended and detrended data, respectively. The results were calculated by averaging over 65°S–90°S in Supplementary Figure 6a for OBS, Supplementary Figure 6b for CON, and Supplementary Figure 7a for CON*. (b) is equivalent to (a) for reanalysis SAT anomalies averaged over Antarctica, excluding the AP region (10°W–270°E, 70°S–90°S) and the AP region (280°E–330°E, 60°S–80°S). (c) is equivalent to (b) for in situ SAT anomalies. The results of (b) and (c) are shown in Supplementary Figure 6c for OBS, Supplementary Figure 6d for CON, and Supplementary Figure 7b for CON*.

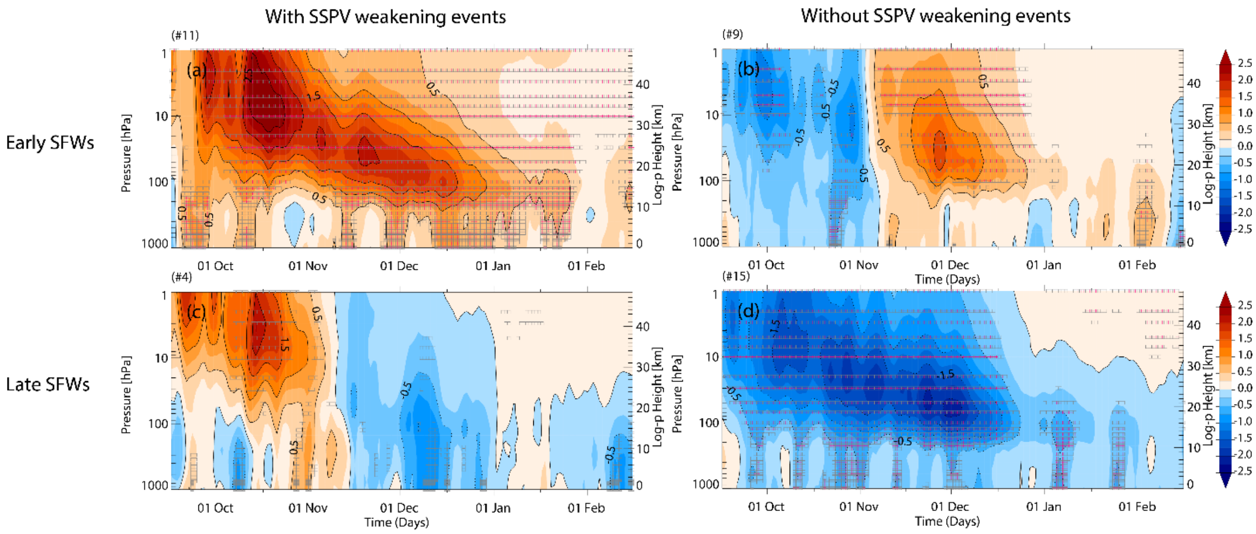

Supplementary Figure 9. Composite of the PCH anomalies according to extreme SSPV weakening events and SFWOD. Composite of the ERA-Interim PCH anomalies based on the calendar day of the year (a) with and (b) without extreme SSPV weakening events for early SFW events. (c, d) are equivalent to (a, b) for late SSW events. SFWOD is referenced in Supplementary Table 4. The number of events used in the composite analysis is indicated in the top left corner of each panel. Pink crosses and gray squares indicate significance at the 95% and 90% confidence levels, respectively.

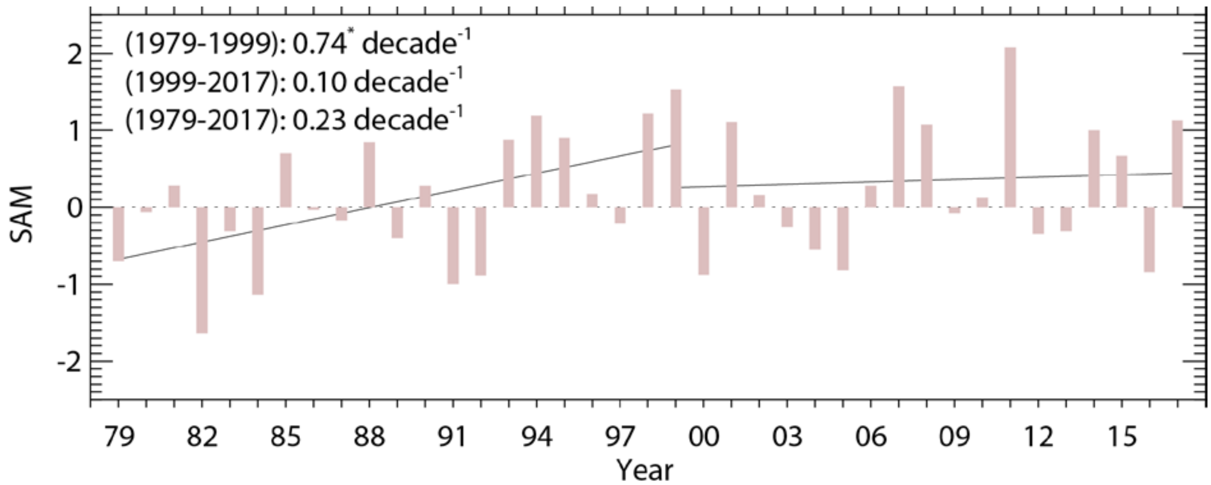

Supplementary Figure 10. Time series of the DJ-mean SAM. The linear trends for the 1979–1999 and 1999–2017 periods are indicated using grey lines. Values in the upper-left corner of the plot represent trends during the three periods. The asterisk indicates significance at the 95% confidence level.

Supplementary Tables

	1998	1999	2000	2001
		SATA (observations)		
Delay	-0.340714	-0.531883**	-0.494240**	-0.423271*
Advance	0.254850	0.198158	-0.123736	-0.245343
Difference	0.595564	0.730041	0.370505	0.177928
		SATA (reanalysis)		
Delay	-0.509751**	-0.725044**	-0.700577**	-0.577017**
Advance	0.109279	0.0919875	-0.265009	-0.427610
Difference	0.619030	0.817032	0.435568	0.149407
		SFWOD		
Delay	8.09774**	10.8312**	8.36815**	9.55534**
Advance	-6.27068	-5.24561	-1.38287	-4.11765
Difference	-14.3684	-16.0768	-9.75102	-13.6730

Supplementary Table 1. Trends in SAT anomalies [ºC decade^{-1}] and SFWOD [day decade^{-1}] and turnaround year testing based on ERA-Interim. Trends and trend differences for different turnaround years. The DJ-mean SAT anomalies and SFWOD trends for the SFWOD-delay era (1979-turnaround year), SFWOD-advance era (turnaround year-2017), and their differences (SFWOD-advance era minus SFWOD-delay era) for turnaround years were defined as 1998, 1999, 2000, and 2001. Single and double asterisks indicate statistical significance at the 90% and 95% confidence levels, respectively.

Early SFW events			Late SFW events		
Number	Year	Onset date	Number	year	Onset date
1	1979	Nov 20	1	1985	Dec 11
2	1980	Nov 22	2	1987	Dec 11
3	1981	Dec 03	3	1990	Dec 14
4	1982	Nov 29	4	1992	Dec 07
5	1983	Dec 05	5	1995	Dec 18
6	1984	Dec 01	6	1996	Dec 15
7	1986	Dec 05	7	1998	Dec 22
8	1988	Nov 18	8	2000	Jan 03
9	1989	Dec 07	9	2001	Dec 25
10	1991	Nov 19	10	2006	Dec 16
11	1993	Dec 06	11	2007	Dec 22
12	1994	Nov 24	12	2008	Dec 24
13	1997	Dec 02	13	2010	Dec 21
14	2000	Nov 26	14	2011	Dec 17
15	2002	Dec 03	15	2014	Dec 12
16	2003	Nov 28	16	2015	Dec 13
17	2004	Nov 27	17	2017	Dec 10
18	2005	Dec 07	18	2020	Dec 27
19	2009	Dec 02	19	2022	Jan 02
20	2012	Nov 19	20	2023	Jan 01
21	2013	Nov 27	-	-	-
22	2016	Nov 20	-	-	-
23	2018	Dec 02	-	-	-
24	2019	Nov 09	-	-	-

Supplementary Table 2. **Onset dates of early and late SFW events based on ERA5.**

Number	Station number	Name	Lat., Lon.
1	89009	Amundsen Scott	-90, 0
2	89050	Bellingshausen	-62.2, 301.1
3	89611	Casey	-66.3, 110.5
4	89571	Davis	-68.6, 78.0
5	89642	Dumont Durville	-66.7, 140.0
6	89063	Faraday\Vernadsky	-65.4, 295.6
7	89022	Halley	-75.5, 333.6
8	89055	Marambio	-64.2, 303.3
9	89056	Marsh	-62.2, 301.1
10	89564	Mawson	-67.6, 62.9
11	89664	McMurdo	-77.9, 166.7
12	89592	Mirny	-66.5, 93.0
13	89512	Novolazarevskaya	-70.8, 11.8
14	89059	O Higgins	-63.3, 302.1
15	88968	Orcadas	-60.7, 315.3
16	89061	Palmer	-64.3, 296
17	89062	Rothera	-67.5, 291.9
18	89066	San Martin	-68.1, 292.9
19	89532	Syowa	-69.0, 39.6
20	00000	Byrd	-80.0, 240.5

Supplementary Table 3. List of in-situ Antarctic stations used in this study.

Early SFW events			Late SFW events		
Number	Year	Onset date	Number	year	Onset date
1	1979	Nov 20	1	1985	Dec 11
2	1980	Nov 22	2	1987	Dec 11
3	1981	Dec 03	3	1989	Dec 07
4	1982	Nov 29	4	1990	Dec 14
5	1983	Dec 06	5	1992	Dec 07
6	1984	Dec 01	6	1995	Dec 19
7	1986	Dec 05	7	1996	Dec 16
8	1988	Nov 19	8	1998	Dec 22
9	1991	Nov 19	9	2000	Jan 03
10	1993	Dec 06	10	2001	Dec 26
11	1994	Nov 24	11	2005	Dec 07
12	1997	Dec 03	12	2006	Dec 16
13	2000	Nov 26	13	2007	Dec 22
14	2002	Dec 03	14	2008	Dec 24
15	2003	Nov 28	15	2010	Dec 21
16	2004	Nov 27	16	2011	Dec 17
17	2009	Dec 02	17	2014	Dec 13
18	2012	Nov 20	18	2015	Dec 13
19	2013	Nov 27	19	2017	Dec 11
20	2016	Nov 20	-	-	-

Supplementary Table 4. Onset dates of early and late SFW events based on ERA-Interim.

Supplementary References

1. H. Kwon, H. Choi, B. M. Kim, S. W. Kim, S. J. Kim, Recent weakening of the southern stratospheric polar vortex and its impact on the surface climate over Antarctica. *Environ. Res. Lett.* **15**, 094072 (2020).